

Fe Isotope Fractionation during Equilibration of Fe–Organic Complexes

JENNIFER L. L. MORGAN,^{*,†}
 LAURA E. WASYLENKI,[‡]
 JOCHEN NUESTER,[§] AND
 ARIEL D. ANBAR^{†,‡}

Arizona State University, Department of Chemistry and Biochemistry, PO Box 871604, Tempe, Arizona 85287, Arizona State University, School of Earth and Space Exploration, PO Box 871404, Tempe, Arizona 85287, and Bigelow Laboratory for Ocean Science, PO Box 475, West Boothbay Harbor, Maine 04575

Received October 1, 2009. Revised manuscript received June 11, 2010. Accepted June 14, 2010.

Despite the importance of Fe–organic complexes in the environment, few studies have investigated Fe isotope effects driven by changes in Fe coordination that involve organic ligands. Previous experimental (Dideriksen et al., 2008, *Earth Planet Sci. Lett.* 269:280–290) and theoretical (Domagal-Goldman et al., 2009, *Geochim. Cosmochim. Acta* 73:1–12) studies disagreed on the sense of fractionation between Fe–desferrioxamine B (Fe–DFOB) and $\text{Fe}(\text{H}_2\text{O})_6^{3+}$. Using a new experimental technique that employs a dialysis membrane to separate equilibrated Fe–ligand pools, we measured the equilibrium isotope fractionations between Fe–DFOB and (1) Fe bound to ethylenediaminetetraacetic acid (EDTA) and (2) Fe bound to oxalate. We observed no significant isotope fractionation between Fe–DFOB and Fe–EDTA ($\Delta^{56/54}\text{Fe}_{\text{Fe–DFOB/Fe–EDTA}} \approx 0.02 \pm 0.11\text{‰}$) and a small but significant fractionation between Fe–DFOB and Fe–oxalate ($\Delta^{56/54}\text{Fe}_{\text{Fe–DFOB/Fe–Ox}_3} = 0.20 \pm 0.11\text{‰}$). Taken together, our results and those of Dideriksen et al. (2008) reveal a strong positive correlation between measured fractionation factors and the Fe-binding affinity of the ligands. This correlation supports the experimental results of Dideriksen et al. (2008). Further, it provides a simple empirical tool that may be used to predict fractionation factors for Fe–ligand complexes not yet studied experimentally.

Introduction

The relative abundances of the four stable isotopes of Fe (^{54}Fe , ^{56}Fe , ^{57}Fe and ^{58}Fe) vary in different environmental materials because the rates and equilibrium constants of many chemical reactions are sensitive to atomic mass (1, 2). With this discovery, the Fe stable isotope system emerged as a powerful new tool to study the sources and chemical transformations of Fe (3–5). It has proven useful in tracking many processes in the environment, including the dissolution of mineral phases, biotic and abiotic redox transformations in modern and ancient settings, and anthropogenic pollution

sources (6–12). The fractionation of Fe and other metal isotopes is strongly affected by the metal bonding environment. However, the relative importance of organic ligand binding for Fe isotope fractionation is not well known.

It is important to understand the effects of organic ligand binding on Fe isotope fractionation because interactions between Fe and organic ligands strongly influence the environmental chemistry and biogeochemistry of this element. In oceans, lakes, and rivers, Fe–organic complexes dominate Fe speciation (13). In aerobic environments where dissolved Fe^{2+} and Fe^{3+} are scarce, some organisms produce low molecular weight organic ligands (siderophores) that stabilize Fe^{3+} in solution and sequester it from other organisms (14). These siderophores have a high binding affinity for Fe^{3+} ($\log K \sim 20\text{--}50$) (15, 16). In addition to siderophores, Fe is also commonly bound to humic and fulvic acids in estuaries, lakes, rivers, and soils.

Ligand interactions unique to Fe may also induce isotope fractionation in biology. The diversity of Fe bonding environments in biomolecules gives rise to its rich biochemistry. Certain Fe motifs are found in many enzymes. These include heme-bound Fe and Fe–sulfur clusters, as well as nonheme Fe coordinated by protein. Differences in Fe–organic coordination among these motifs may induce Fe isotope fractionations manifested in the environment.

Some Fe isotope variations in nature have already been attributed to Fe–organic ligand complexation (17, 18). For example, isotope fractionation associated with organic complexation may explain why dissolved Fe in the organic-rich tributaries of the Negro River is enriched in heavy Fe isotopes (18). However, the validity of such interpretations is uncertain because there have been few experimental or theoretical studies of Fe isotope fractionation during interaction with organic ligands (8, 9, 19–23). With over 500 known siderophore complexes (13) and numerous other Fe-binding molecules in the environment, a systematic understanding of Fe isotope fractionation during ligand binding is required.

Among the studies that do exist, there are significant discrepancies between experimental assessments and theoretical predictions of Fe isotope fractionation involving organic ligands. The first measurement of the equilibrium isotope fractionation between Fe^{3+} bound to the siderophore desferrioxamine B (DFOB) and the inorganic Fe complex $\text{Fe}(\text{H}_2\text{O})_6^{3+}$ indicated a fractionation of $\sim 0.6\text{‰}$ ($\delta^{56/54}\text{Fe}_{\text{sample}} = ((^{56}\text{Fe}/^{54}\text{Fe})_{\text{sample}} / ((^{56}\text{Fe}/^{54}\text{Fe})_{\text{IRMM-014}}) - 1) \times 1000$), favoring heavier isotopes in the Fe^{3+} –DFOB complex (22). This effect is significant compared to the total range of Fe isotope variation found in nature ($\sim 3\text{‰}$) (4). In contrast, theoretical calculations using molecular orbital/density functional theory (MO/DFT) for the same equilibrium reaction, including water solvation and at 25 °C, predicted an isotope effect of 0.3‰ in the opposite direction, favoring lighter isotopes in the Fe^{3+} –DFOB complex (20). This disagreement between experimental and theoretical findings suggests shortcomings in either prior experiments or MO/DFT computations.

Here we present determinations of the magnitude and direction of equilibrium Fe isotope fractionation involving the Fe–organic complexes Fe^{3+} –DFOB, Fe^{3+} –oxalate (Fe^{3+} – Ox_3), and Fe^{3+} –ethylenediaminetetraacetic acid (Fe^{3+} –EDTA), using a new experimental method. We compare these data to prior experimental and theoretical results.

Experimental and Analytical Methods

Experimental Design. We utilized a new method to measure equilibrium isotope fractionation. In the approach employed previously by Dideriksen et al. (22), $\text{Fe}(\text{H}_2\text{O})_6^{3+}$ was separated

* Corresponding author phone: 480-727-8284; fax: 480-965-8102; e-mail: jennifer.l.morgan@asu.edu.

[†] Department of Chemistry and Biochemistry.

[‡] School of Earth and Space Exploration.

[§] Bigelow Laboratory for Ocean Science.

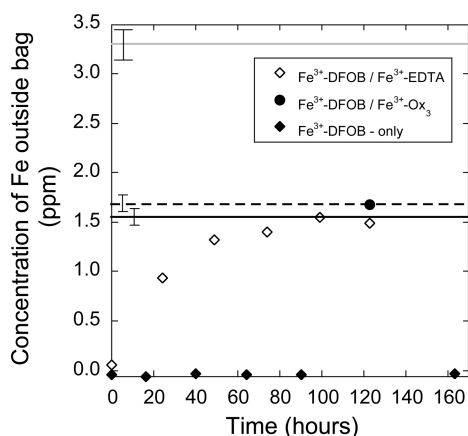


FIGURE 1. The horizontal lines shown represent the expected Fe concentrations outside the bag if either one ligand (solid black line, and dashed black line), or both ligands (solid gray line), escaped the bag from the two mixed-ligand experiments. The error bars on the horizontal lines represent 5% standard deviation as defined by replicate measurements of standards. Three separate dialysis bag experiments were performed. In experiment 1, 3 mL of 5 mM Fe (280 ppm Fe) as Fe^{3+} -DFOB/ Fe^{3+} -EDTA were added to a dialysis bag (solid black line, open diamonds). In experiment 2, 3 mL of 5 mM Fe as Fe^{3+} -DFOB/ Fe^{3+} - Ox_3 were placed into a dialysis bag (dashed black line, closed circle). In experiment 3, 3 mL of 5 mM Fe as Fe^{3+} -DFOB were added (closed diamonds). Each bag was placed in 250 mL jars of 18 $\text{M}\Omega$ water, and the Fe concentration outside the bag was measured over time using the Ferrozine[®] method. Concentrations in all cases indicate that Fe^{3+} -DFOB was trapped by the membrane, while Fe^{3+} -EDTA and Fe^{3+} - Ox diffused to the outside. For the time series concentration measurements the error bars are smaller than the symbols.

from Fe^{3+} -DFOB after equilibration by rapidly increasing pH, resulting in rapid (<1 s) precipitation of $\text{Fe}(\text{H}_2\text{O})_6^{3+}$ as Fe-oxyhydroxide. After separating the solution and precipitate by centrifugation, the isotope compositions of both Fe pools were measured. However, the precipitation of Fe-oxyhydroxides can induce an isotope effect of its own (12). In order to check for this potential problem and to correct for its effects, it is necessary to measure the rate of precipitation, the isotope composition of the remaining $\text{Fe}(\text{H}_2\text{O})_6^{3+}$ pool, and the rate of isotope exchange between $\text{Fe}(\text{H}_2\text{O})_6^{3+}$ and Fe^{3+} -DFOB. This was accomplished via parallel sets of control experiments with a ^{57}Fe tracer. Further, this method of separation is only applicable when one of the equilibrating species is $\text{Fe}(\text{H}_2\text{O})_6^{3+}$, limiting the utility when considering pairs of organic species.

Membrane separations offer an alternative to precipitation and centrifugation in isotope equilibration studies. For example, in a study of Zn isotopes, a Donnan membrane was used to separate Zn^{2+} from Zn^{2+} bound to purified humic acid (24). However, because the Donnan membrane requires that one of the equilibrating species be charged, it cannot be used for studies involving neutral organic species.

Dialysis membranes offer another possibility. In our study, dialysis bags with a nominal molecular weight cutoff of 100 g/mol were used to physically separate the Fe ligand pools by simple diffusion. We determined experimentally that the actual molecular weight cutoff was variable. In the experiments reported here, the bags allowed small ligand complexes of up to 350 g/mol to diffuse through, while ligand complexes heavier than 350 g/mol were unable to cross the membrane (Figure 1). The exact molecular weight cutoff varied among bags purchased at different times either as a result of subtle manufacturing variations in different batches of bags or of

pore size changing with age. Control experiments involving one Fe-ligand complex in the dialysis bag were performed with new bag batches and for every Fe-ligand complex to ensure successful separation.

Two sets of experiments were conducted for each ligand pair: one with ^{54}Fe tracer to quantify the extent of isotope exchange and one with "normal" Fe (~0‰) to measure isotope fractionation. In a typical experiment, two Fe-ligand stock solutions were prepared, mixed, allowed to equilibrate for at least 24 h, then placed in a 3 mL dialysis bag. The bag was placed inside a 250 mL jar of 18 $\text{M}\Omega$ -cm water, which was agitated to facilitate diffusion of the smaller ligand through the bag and into the surrounding solution. Samples were taken from both the inside solution and the outside solution for isotope analyses.

The experiments were designed so that approximately half the Fe would be bound in the larger siderophore complex, DFOB, and half would be bound to the smaller ligand, EDTA or Ox_3 , based on equilibrium constants obtained from the literature (Table 1). The Fe concentrations outside the bags were monitored in every experiment to ensure that the concentration reached the value expected if only the smaller Fe complex diffused out and attained uniform concentration on both sides of the membrane (Figure 1).

The advantages of the dialysis bag method over precipitation are (a) there is no back reaction requiring correction; and (b) our separation method can be used even when $\text{Fe}(\text{H}_2\text{O})_6^{3+}$ is not one of the equilibrating species (22).

Experimental Details. Stock solutions were made for multiple experiments. The ^{54}Fe -DFOB stock solution was made by mixing 5.2 mM DFOB (Fisher Scientific desferrioxamine mesylate) and 5.1 mM ^{54}Fe (lot no. 166642, Oak Ridge National Laboratories, FeCl_3 in 2% HNO_3 ; ^{54}Fe (96.41%), ^{56}Fe (3.49%), ^{57}Fe (0.10%), ^{58}Fe (<0.03%)). The Fe-EDTA stock solution contained 5.10 mM EDTA (Acros Organics ethylenediaminetetraacetic acid, 99%) and 5.1 mM Fe (Fisher Scientific, FeCl_3 in 2% HNO_3). The Fe- Ox_3 solution contained 15.4 mM oxalic acid (Fisher Chemical oxalic acid) and 5.1 mM Fe. The Fe-DFOB solution contained 5.1 mM DFOB and 5.2 mM Fe. All solutions were made with 18.2 $\text{M}\Omega$ -cm water and kept at room temperature.

The tracer experiments were performed by mixing 7.5 mL of $^{54}\text{Fe}^{3+}$ -DFOB stock with 7.5 mL of Fe^{3+} -EDTA or Fe^{3+} - Ox_3 . The equilibrium experiments were performed by mixing 7.5 mL of Fe^{3+} -DFOB stock with 7.5 mL of Fe^{3+} -EDTA or Fe^{3+} - Ox_3 . For all experiments, the initial pH was 3. After 24 h of equilibration, 3 mL was transferred to a dialysis bag (Spectrum Lab, 100D CE Float-A-Lyzer). The bag and its contents were placed in a jar containing 250 mL of 18 $\text{M}\Omega$ -cm water freshly extracted from a DI system, with an initial pH of 7. In all experiments, pH decreased to 5. In the case of Fe^{3+} - Ox_3 , the experiment was kept in an amber colored shaker while being agitated, or in a dark cabinet, to prevent photoreduction of Fe^{3+} - Ox_3 (25).

Once each experiment reached completion, as assessed in near real-time using UV-vis spectrophotometry and Ferrozine with hydroxylamine reagent (26), the bag was removed from the surrounding solution. The concentration of Fe in the surrounding solution was then analyzed using ICP-MS to quantify mass balance (Table 2). The inside solution was diluted from 3 mL (initial volume) to 3.5–5 mL because of osmosis. The final volume was used to calculate the μg of Fe in the experiment to assess mass balance. Fe mass balance was achieved within analytical error ($2\sigma = \pm 5\%$) for all experiments (Table 3). This indicates that significant sorption to the dialysis membrane did not occur. It also indicates that in the unlikely event of bacterial growth, there was no significant biotic removal of Fe from solution. While a small amount of the diffusing Fe-ligand complex remained inside the bag (~1%), its contribution to the Fe

TABLE 1. Binding Affinities and Formula Weights for Organic Ligands^a

ligand	log (<i>K</i>)	formula weight
Fe–desferrioxamine-B (DFOB)	31	617 g/mol
Fe–ethylenediaminetetraacetic acid (EDTA)	25	348 g/mol
Fe–oxalate (Ox ₃)	19	326 g/mol (for 3 ligands)

^a From Martell and Smith (30).

TABLE 2. Iron Concentrations and $\delta^{56/54}\text{Fe}$ in Experimental Solutions

solution	measured [Fe, ppm] $2\sigma = \pm 5\%$	$\delta^{56/54}\text{Fe}$ (‰) $\pm 2\sigma, n = 3-4$
stock		
⁵⁴ Fe ³⁺ –DFOB	300.0	-91.77 ± 0.03
Fe ³⁺ –EDTA	281.2	0.26 ± 0.09
Fe ³⁺ –Ox ₃	299.9	0.20 ± 0.06
Fe ³⁺ –DFOB	272.4	0.23 ± 0.13
spike Fe		
⁵⁴ Fe ³⁺ –DFOB/Fe ³⁺ –Ox ₃ mixture	299.9	-48.26 ± 0.11
inside (Fe ³⁺ –DFOB)	120.9	-48.32 ± 0.11
outside (Fe ³⁺ –Ox ₃)	1.6	-48.27 ± 0.07
⁵⁴ Fe ³⁺ –DFOB/Fe ³⁺ –EDTA mixture	290.6	-48.12 ± 0.08
inside (Fe ³⁺ –DFOB)	147.8	-48.39 ± 0.09
outside (Fe ³⁺ –EDTA)	1.7	-47.86 ± 0.08
normal Fe		
Fe ³⁺ –DFOB/Fe ³⁺ –Ox ₃ Mixture	286.2	0.24 ± 0.03
inside (Fe ³⁺ –DFOB)	87.6	0.25 ± 0.10
outside (Fe ³⁺ –Ox ₃)	1.6	0.05 ± 0.06
Fe ³⁺ –DFOB/Fe ³⁺ –EDTA mixture	276.8	0.25 ± 0.05
inside (Fe ³⁺ –DFOB)	82.8	0.17 ± 0.07
outside (Fe ³⁺ –EDTA)	1.4	0.15 ± 0.09

TABLE 3. Added and Measured Iron Quantities in the Experiments; $\mu\text{g Fe}$ in Experiment ($2\sigma = \pm 5\%$)

solution	$\mu\text{g Fe}$ added	$\mu\text{g Fe}$ measured (inside and outside bag)
spike Fe		
⁵⁴ Fe ³⁺ –DFOB/Fe ³⁺ –Ox ₃ mixture	757	724
⁵⁴ Fe ³⁺ –DFOB/Fe ³⁺ –EDTA mixture	815	848
normal Fe		
Fe ³⁺ –DFOB/Fe ³⁺ –Ox ₃ mixture	839	804
Fe ³⁺ –DFOB/Fe ³⁺ –EDTA mixture	803	806

isotope composition of the inside solution was negligible. The high recovery of the smaller and less stable Fe–ligands also shows that significant quantities of Fe–oxyhydroxides, which would have remained in the bag, did not form.

Aliquots of the inside and outside solutions were taken to obtain 14 μg of Fe for each isotopic analysis: $\sim 145 \mu\text{L}$ from the inside solution and $\sim 11.8 \text{ mL}$ from the outside solution. These aliquots were dried and digested using distilled HNO_3 and ultrapure H_2O_2 . Once digested, the samples were diluted in 0.32 M HNO_3 for analysis. Typically, for Fe isotope analysis samples must be chemically purified using anion exchange resin to isolate Fe from other elements. However, chemical purification of these experimental samples was not needed because the sample matrix only contains Fe and easily digested organic ligands.

Analytical Procedures. Precise Fe concentrations were measured by quadrupole ICP-MS (Thermo Scientific X Series). Sample and standard solutions were introduced in parallel with an internal standard solution containing yttrium

for normalization of plasma variation. Uncertainties for replicate measurements were approximately $\pm 5\%$ (2σ).

Fe isotope compositions were measured following the method of Arnold et al. using a multiple collector ICP-MS (Thermo Scientific Neptune) (27). Medium mass-resolution mode (50 μm slits) was used to resolve the polyatomic interferences $^{40}\text{Ar}^{16}\text{O}^+$, and $^{40}\text{Ar}^{14}\text{N}^+$ and $^{40}\text{Ar}^{16}\text{OH}^+$ from $^{54}\text{Fe}^+$, $^{56}\text{Fe}^+$ and $^{57}\text{Fe}^+$, respectively (28). We monitored mass 53 for ^{53}Cr to ensure that there was no interference from ^{54}Cr , although our experimental system nominally contains no Cr. Some samples were measured using high mass-resolution mode (25 μm slits) when medium resolution slits were unavailable; other than reducing the ion beam intensities and hence requiring less diluted samples, the use of high mass-resolution slits had no effect on our data. The Fe concentrations of samples and standards were 600 ppb (10.74 μM) for medium resolution analyses and 1200 ppb (21.48 μM) for high resolution analyses. Sample and standard concentrations were checked during the analysis to ensure

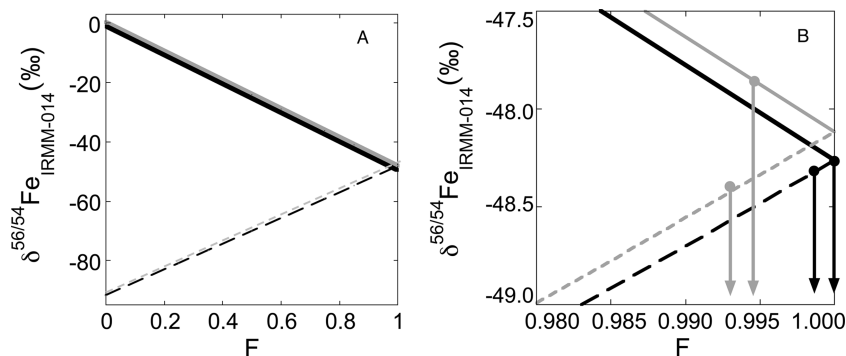


FIGURE 2. A) Expected isotope composition as a function of isotope exchange progress. The lines were calculated using equations 2 and 3 then converted to F . F is the fractional extent to which exchange has approached completion. $F = 0$ indicates no exchange occurs. $F = 1$ indicates complete exchange between pools. The black solid line is $\text{Fe}^{3+}\text{-Ox}_3$, and the dashed black line is $^{54}\text{Fe}^{3+}\text{-DFOB}$ mixed with $\text{Fe}^{3+}\text{-Ox}_3$. The solid gray line is $\text{Fe}^{3+}\text{-EDTA}$, and the dashed gray line is $^{54}\text{Fe}^{3+}\text{-DFOB}$ mixed with $\text{Fe}^{3+}\text{-EDTA}$. B) Magnified view of $F > 0.980$. The points on the line show the measured isotope composition of each ligand after the experiment. The arrows show the extent to which the ligands mixed in each experiment. Each was $>99\%$ mixed.

they were identical to within $\pm 5\%$. Instrumental mass bias, that is, isotope fractionation produced by the mass spectrometer, was corrected using a combination of standard-sample bracketing and addition of Cu as an internal standard (27). Cu concentrations matched Fe concentrations in all standards and samples.

For each isotopic analysis, 20 cycles with 16.77 s integrations were averaged. Three isotope ratios were measured simultaneously: $^{56}\text{Fe}/^{54}\text{Fe}$, $^{57}\text{Fe}/^{54}\text{Fe}$, and $^{58}\text{Fe}/^{54}\text{Fe}$. All ratios were measured relative to the IRMM-014 standard (Institute of Reference Material and Measurement, Geel, Belgium). Values are reported as follows:

$$\delta^{56/54}\text{Fe}_{\text{sample}} = \left(\frac{(^{56}\text{Fe}/^{54}\text{Fe})_{\text{sample}}}{(^{56}\text{Fe}/^{54}\text{Fe})_{\text{IRMM-014}}} - 1 \right) \times 1000 \quad (1)$$

As a quality-control measure, we checked that all measured isotope values obeyed mass dependence by comparing $\delta^{56/54}\text{Fe}$ and $\delta^{57/54}\text{Fe}$ (the precision of $\delta^{56/54}\text{Fe}$ was typically too poor to be useful, due to the relative rarity of ^{58}Fe). Data were rejected if $\delta^{56/54}\text{Fe}/2$ differed from $\delta^{57/54}\text{Fe}/3$ by more than 0.05% (this check was not applicable to isotope tracer experiments). Data were also rejected if the magnitude of the mass bias correction exceeded 0.35% . Good agreement between $\delta^{56/54}\text{Fe}/2$ and $\delta^{57/54}\text{Fe}/3$, as well as small instrumental mass bias corrections, indicate that the isotope measurements were not significantly affected by interferences or other matrix effects. Data were rejected if the ion beam intensity from $^{56}\text{Fe}^+$ was < 6 V, because in such cases the contribution of instrument blank to the beam intensities measured for the less abundant Fe isotopes becomes significant.

Solutions containing extreme enrichments of ^{54}Fe , used in tracer experiments, were usually run at the end of an analytical session to avoid any chance of memory effects. However, no such effects were seen when running standards immediately after such samples.

Throughout the analytical runs, we measured the IRMM-014 standard, gravimetric standards of known isotope composition, and previously analyzed rock standards to ensure accuracy and reproducibility from session to session. Based on replicate measurements of each sample, the external precision was better than $\pm 0.11\%$ ($\pm 2\sigma$) in $\delta^{56/54}\text{Fe}$.

Results and Discussion

Verification of Isotope Equilibration. We assessed the extent of isotope equilibration in ^{54}Fe tracer experiments. The isotope compositions of all solutions and mixtures were measured directly so as to not assume an isotope composition

based on a mixing calculation. The initial isotope composition of $^{54}\text{Fe}^{3+}\text{-DFOB}$ in these tracer experiments was $\delta^{56/54}\text{Fe} = -91.77 \pm 0.03\%$. The initial isotope compositions of $\text{Fe}^{3+}\text{-EDTA}$ and $\text{Fe}^{3+}\text{-Ox}_3$ were $0.26 \pm 0.09\%$ and $0.20 \pm 0.06\%$ ($\delta^{56/54}\text{Fe}$). The isotope compositions of the $\text{Fe}^{3+}\text{-DFOB}$ /ligand mixtures were $-48.12 \pm 0.08\%$ and $-48.26 \pm 0.11\%$ for $\text{Fe}^{3+}\text{-EDTA}$ and $\text{Fe}^{3+}\text{-Ox}_3$, respectively. After separating the complexes, the isotope composition of Fe inside the bag ($\text{Fe}^{3+}\text{-DFOB}$) was $-48.39 \pm 0.09\%$ after exchange with $\text{Fe}^{3+}\text{-EDTA}$ and $-48.32 \pm 0.11\%$ after exchange with $\text{Fe}^{3+}\text{-Ox}_3$. The Fe isotope composition outside the bag for $\text{Fe}^{3+}\text{-EDTA}$ was $-47.86 \pm 0.08\%$. The Fe isotope composition for $\text{Fe}^{3+}\text{-Ox}_3$ was $-48.27 \pm 0.07\%$ (Table 2).

The isotopes in both experiments converge toward a common value, indicating that the isotopes exchanged between the two Fe–ligand complexes. The isotope composition that should be attained after complete equilibration is easily predicted by mass balance. The isotope compositions of the separated ligands can be predicted using the following equations:

$$\delta^{56/54}\text{Fe}_{\text{DFOB-final}} = (1 - M) \delta^{56/54}\text{Fe}_{\text{DFOB-initial}} + M \delta^{56/54}\text{Fe}_{\text{unspikedligand-initial}} \quad (2)$$

$$\delta^{56/54}\text{Fe}_{\text{unspikedligand-final}} = (1 - M) \delta^{56/54}\text{Fe}_{\text{unspikedligand-initial}} + M \delta^{56/54}\text{Fe}_{\text{DFOB-initial}} \quad (3)$$

Here, M is the fraction of Fe in each complex that has exchanged with the other complex. Since no more than 52.7% of the Fe came from $^{54}\text{Fe}^{3+}\text{-DFOB}$, M must be $0 \leq M \leq 0.527$. M can be converted to F , the percent exchanged, by dividing M obtained from Equation 2 and Equation 3 by the percent Fe that was initially added to the experiment from $\text{Fe}^{3+}\text{-unspikedligand}$ and $^{54}\text{Fe}^{3+}\text{-DFOB}$, respectively. Equations 2 and 3 are approximations, but these approximations deviate from the actual equivalence by no more than 1% as long as $\delta^{56/54}\text{Fe}_{\text{spike}} - \delta^{56/54}\text{Fe}_{\text{unspiked}} < 400\%$ (29). The Fe isotope composition of each Fe–ligand complex is shown as a function of F in Figure 2A.

When the measured isotope values are substituted into eq 1 and 2, the results indicate that $>99\%$ of the Fe exchanged in all experiments (Figure 2B). These results demonstrate that despite the strong binding affinity of DFOB for Fe, Fe isotopes exchange between DFOB and ligands with smaller Fe-binding affinities. The extent of exchange also indicates that the experiments closely approached equilibrium.

Equilibrium Isotope Fractionation. Isotope fractionation between pairs of organic Fe complexes was measured using

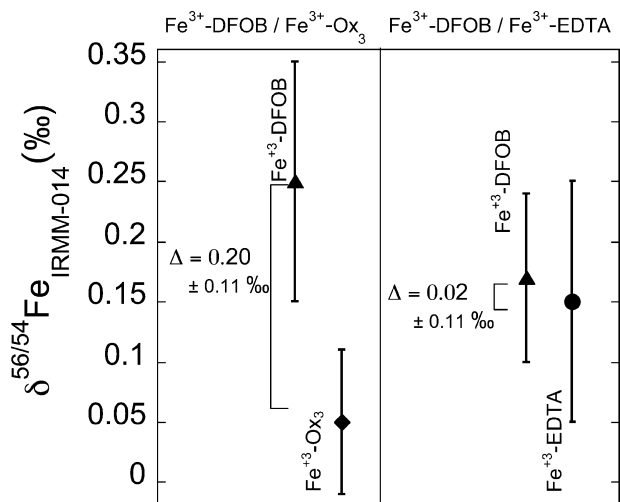


FIGURE 3. Measured $\delta^{56/54}\text{Fe}$ for each sample. $\text{Fe}^{3+}\text{-DFOB}$ and $\text{Fe}^{3+}\text{-Ox}_3$ were significantly different with $\Delta^{56/54}\text{Fe} = 0.20 \pm 0.11\text{‰}$. $\text{Fe}^{3+}\text{-DFOB}$ and $\text{Fe}^{3+}\text{-EDTA}$ were within analytical error of each other, indicating that $\Delta \approx 0.02 \pm 0.11\text{‰}$. Error bars represent $\pm 2\sigma$ uncertainty on replicate measurements of samples.

the same procedures described above, but beginning with $\text{Fe}^{3+}\text{-DFOB}$, $\text{Fe}^{3+}\text{-EDTA}$, and $\text{Fe}^{3+}\text{-Ox}_3$ of the same initial Fe isotope composition (these experiments had no ^{54}Fe tracer). By measuring $\delta^{56/54}\text{Fe}$ in the separated ligand pools after equilibration, we found that the fractionation between $\text{Fe}^{3+}\text{-DFOB}$ and $\text{Fe}^{3+}\text{-Ox}_3$ ($\Delta^{56/54}\text{Fe}_{\text{Fe-DFOB/Fe-Ox}_3} = \delta^{56/54}\text{Fe}_{\text{Fe-DFOB}} - \delta^{56/54}\text{Fe}_{\text{Fe-Ox}_3}$) is $0.20 \pm 0.11\text{‰}$, while the difference between $\text{Fe}^{3+}\text{-DFOB}$ and $\text{Fe}^{3+}\text{-EDTA}$ is $0.02 \pm 0.11\text{‰}$ (Figure 3). These values indicate that organic ligand binding affects the magnitude of Fe isotope fractionation.

We cannot directly compare our results with those of Dideriksen et al. (22) because it was not possible to use our experimental method to directly measure the fractionation between $\text{Fe}^{3+}\text{-DFOB}$ and $\text{Fe}(\text{H}_2\text{O})_6^{3+}$; to avoid precipitation of hydrous ferric oxides from $\text{Fe}(\text{H}_2\text{O})_6^{3+}$, pH would need to be <3 , causing the dialysis membrane to degrade. However, an indirect comparison is possible if we plot $\Delta^{56/54}\text{Fe}$ as a function of the affinity constants ($\log K$) of the Fe-binding ligands. The assumption underlying this simple, first-order comparison is that Fe isotope fractionation in these systems is largely driven by differences in Fe–ligand binding affinity between the equilibrating complexes. Specifically, we plot $\Delta^{56/54}\text{Fe}$ versus $\Delta \log K$ (Figure 4), where $\Delta \log K$ is the difference in $\log K$ values between the two equilibrating species. In the case of isotope exchange between $\text{Fe}(\text{H}_2\text{O})_6^{3+}$ and $\text{Fe}^{3+}\text{-DFOB}$, $\Delta \log K$ is simply the binding affinity for the reaction $\text{Fe}^{3+} + \text{DFOB} \rightarrow \text{Fe}^{3+}\text{-DFOB}$, because the value of this $\log K$ was determined in an aqueous solution in which Fe^{3+} was presumably present as the hexaquo complex (30).

When our results are combined with those of Dideriksen et al. (22) in this way, a linear trend emerges (Figure 4). This trend follows the expectation that heavier isotopes preferentially partition into stronger bonding environments and that the magnitude of this effect scales with differences in bond strengths (31, 32). (Note that this relationship only applies to ligands in equilibrium with each other and does not account for kinetic isotope effects.)

Our findings are consistent with other recent work. Ottonello and Zuccolini (23) similarly suggested a positive correlation between Fe–ligand binding affinity and equilibrium isotope fractionation based on their MO/DFT study of consecutive binding of acetic acid molecules to Fe^{3+} . Wiederhold et al. (21) and Brantley et al. (9) observed light

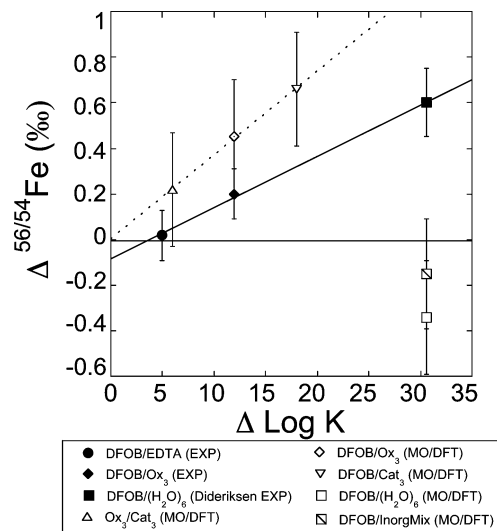


FIGURE 4. Plot of isotope fractionation as a function of the difference in $\log K$ for each ligand pair. The linear trend based on experiments has a slope of 0.02 ± 0.005 . The y-intercept is 0.08 ± 0.08 . The uncertainties on the slope and y-intercept were calculated using Isoplot (35). The experimental results fall on a line with an R^2 value of 0.99. The error bars are propagated 2σ uncertainties on replicate measurements. The MO/DFT predictions for $\text{Fe}^{3+}\text{-Ox}_3/\text{Fe}^{3+}\text{-Cat}_3$, $\text{Fe}^{3+}\text{-DFOB}/\text{Fe}^{3+}\text{-Ox}_3$, and $\text{Fe}^{3+}\text{-DFOB}/\text{Fe}^{3+}\text{-Cat}_3$ are plotted as a function of the difference in $\log K$. The MO/DFT predictions form a linear trend that is offset and has a different slope from the experimental trend (see the Reconciling Experiments and Theory section).

Fe bound to ligands with high Fe binding affinity in leaching experiments with goethite and hornblende, respectively, but these experiments were not at equilibrium, and thus an opposite sense of fractionation from our experiments is unsurprising. Wiederhold's long-duration experiments displayed an isotopically heavy product and therefore likely represent equilibrium exchange between goethite-bound Fe and oxalate-bound Fe with a fractionation of $0.5 \pm 0.15\text{‰}$ (21). There is no simple Fe binding affinity constant for the goethite lattice, but this result suggests a stronger bonding environment for Fe in $\text{Fe}^{3+}\text{-Ox}_3$ than for Fe in goethite.

Reconciling Experiments and Theory. To assess the validity of the experimental trend of $\Delta^{56/54}\text{Fe}$ versus $\Delta \log K$, we plotted the theoretically predicted $\Delta^{56/54}\text{Fe}$ values for $\text{Fe}^{3+}\text{-Ox}_3/\text{Fe}^{3+}\text{-catecholate (Cat}_3)$, $\text{Fe}^{3+}\text{-DFOB}/\text{Fe}^{3+}\text{-Ox}_3$, and $\text{Fe}^{3+}\text{-DFOB}/\text{Fe}^{3+}\text{-Cat}_3$ (19) as a function of the difference in $\log K$ (Figure 4). Like the experimental results, these MO/DFT predictions form a linear trend. This trend in theoretical $\Delta^{56/54}\text{Fe}$ versus $\Delta \log K$ supports our observation that the extent of fractionation correlates directly with differences in binding affinity. However, the two trend lines are slightly offset and have different slopes. These differences suggest that MO/DFT calculations may systematically deviate from experimental fractionation factors, and that this problem may worsen with increasing difference in $\log K$. Experiments that directly quantify the fractionation factors for $\text{Fe}^{3+}\text{-Ox}_3/\text{Fe}^{3+}\text{-Cat}_3$, and $\text{Fe}^{3+}\text{-DFOB}/\text{Fe}^{3+}\text{-Cat}_3$ could test this suggestion.

Our findings and interpretations shed new light on the mismatch between previous experimental and theoretical studies of fractionation between $\text{Fe}^{3+}\text{-DFOB}$ and $\text{Fe}(\text{H}_2\text{O})_6^{3+}$. The previous study that measured Fe in equilibrium between siderophore ($\text{Fe}^{3+}\text{-DFOB}$) and inorganic Fe complex ($\text{Fe}(\text{H}_2\text{O})_6^{3+}$) reported a fractionation of $\sim 0.6\text{‰}$ ($\Delta^{56/54}\text{Fe}$), favoring heavier isotopes in the $\text{Fe}^{3+}\text{-DFOB}$ complex (22).

The corresponding quantum chemical calculations for the same system predicted an isotope effect of 0.3‰ in the opposite direction (20). In an attempt to more accurately model speciation in experiments prior to and during precipitation, Domagal-Goldman et al. (20) modeled a mixture of inorganic species ($\text{Fe}(\text{H}_2\text{O})_6^{3+}$, $\text{Fe}(\text{H}_2\text{O})_8(\text{OH})_2^{3+}$ and $\text{Fe}(\text{H}_2\text{O})_6^{2+}$). This modification changed the isotope fractionation to -0.15‰ , but did not fully resolve the disagreement with experiments. Neither of these calculated values for $\text{Fe}(\text{H}_2\text{O})_6^{3+}$ in equilibrium with Fe^{3+} -DFOB falls on the linear trend defined by experiments, or on the trend defined by the other MO/DFT calculations (Figure 4).

Similar discrepancies were noted between experimental and theoretical fractionation factors observed between $\text{Fe}(\text{H}_2\text{O})_6^{3+}$ and a series of mineral phases (20). There is an average offset of 0.8‰ between the experimental and theoretical values for these systems. The theoretical calculations predict that $\text{Fe}(\text{H}_2\text{O})_6^{3+}$ should be enriched in heavy isotopes compared to the mineral phase, but this is not observed in experiments (19). The discrepancies between experiments and theory are consistently of similar magnitude and in the same direction when $\text{Fe}(\text{H}_2\text{O})_6^{3+}$ is involved. We hypothesize that there is a specific deficiency in MO/DFT models of $\text{Fe}(\text{H}_2\text{O})_6^{3+}$.

Broader Implications. The linear trend we observe between $\Delta^{56/54}\text{Fe}$ and $\Delta\log K$ may prove particularly useful in predicting equilibrium isotope fractionation induced by ligands that have not been experimentally tested or theoretically modeled. For example, the equilibrium Fe isotope fractionation for Fe^{3+} -DFOB in equilibrium with Fe^{3+} -citrate has not been measured or modeled. The difference in binding affinity between Fe^{3+} -DFOB and Fe^{3+} -citrate is 19.2. Using the linear trend we predict a fractionation of $\Delta^{56/54}\text{Fe}_{\text{Fe-DFOB/Fe-citrate}} = 0.33 \pm 0.26\text{‰}$. Future experimental work could test this hypothesis.

More broadly, our results confirm that isotope fractionations generated from interactions between Fe and organic ligands can be significant and are therefore likely to be important in natural systems. Because many different types of ligands bind Fe in nature, improved understanding of the systematics of ligand-driven isotope effects may prove particularly useful in studying weathering, biological acquisition and metabolism of Fe. Iron cycling in these systems often involves Fe redox changes, which cause some of the largest known Fe isotope fractionations (33, 34). The presence of organic ligands, especially those that have high affinity for only one redox state of Fe, could be important in governing Fe isotope signatures in natural systems.

Acknowledgments

Funding for this project was provided by NSF-EAR 0519347 to A.D.A. and L.E.W. NASA Astrobiology institute supported some of our time. We thank Gwyneth Gordon for helping with analyses and Sue Brantley for inspiring discussions. The authors would also like to thank all 4 anonymous reviewers for their help and advice.

Literature Cited

- Johnson, C. M.; Beard, B. L.; Roden, E. E. The iron isotope fingerprints of redox and biogeochemical cycling in modern and ancient Earth. *Annu. Rev. Earth Planet Sci.* **2008**, *36*, 457–493.
- Anbar, A.; Rouxel, O. Metal stable isotopes in paleoceanography. *Annu. Rev. Earth Planet Sci.* **2007**, *35*, 717–746.
- Beard, B. L.; Johnson, C. M.; Cox, H.; Neelson, K. H.; Aguilar, C. Iron isotope biosignatures. *Science* **1999**, *285* (5435), 1889–1892.
- Anbar, A. D. Iron stable isotopes: beyond biosignatures. *Earth Planet Sci. Lett.* **2004**, *217* (3–4), 223–236.
- Fehr, M. A.; Andersson, P. S.; Halenius, U.; Morth, C. Iron isotope variations in Holocene sediments of the Gotland Deep, Baltic Sea. *Geochim. Cosmochim. Acta* **2008**, *72* (3), 807–826.

- Beard, B. L.; Johnson, C. M.; Skulan, J. L.; Neelson, K. H.; Cox, L.; Sun, H. Application of Fe isotopes to tracing the geochemical and biological cycling of Fe. *Chem. Geol.* **2003**, *195* (1–4), 87–117.
- Flament, P.; Mattielli, N.; Aimo, L.; Choel, M.; Deboudt, K.; de Jong, J.; Rimetz-Planchon, J.; Weis, D. Iron isotopic fractionation in industrial emissions and urban aerosols. *Chemosphere* **2008**, *73* (11), 1793–1798.
- Brantley, S. L.; Liermann, L.; Bullen, T. D. Fractionation of Fe isotopes by soil microbes and organic acids. *Geology* **2001**, *29* (6), 535–538.
- Brantley, S. L.; Liermann, L. J.; Gwynn, R. L.; Anbar, A.; Icopini, G. A.; Barling, J. Fe isotopic fractionation during mineral dissolution with and without bacteria. *Geochim. Cosmochim. Acta* **2004**, *68* (15), 3189–3204.
- Walczyk, T.; von Blanckenburg, F. Deciphering the iron isotope message of the human body. *Int. J. Mass Spectrom.* **2005**, *242* (2–3), 117–134.
- Majestic, B. J.; Anbar, A. D.; Herckes, P. Stable isotopes as a tool to apportion atmospheric iron. *Environ. Sci. Technol.* **2009**, *43*, 4327–4333.
- Johnson, C. M.; Skulan, J. L.; Beard, B. L.; Sun, H.; Neelson, K. H.; Braterman, P. S. Isotopic fractionation between Fe(III) and Fe(II) in aqueous solutions. *Earth Planet Sci. Lett.* **2002**, *195* (1–2), 141–153.
- Raymond, K. N.; Carrano, C. J. Coordination chemistry and microbial iron transport. *Acc. Chem. Res.* **1979**, *12* (5), 183–190.
- Hutchins, D.; Witter, A.; Butler, A.; Luther III, G. Competition among marine phytoplankton for different chelated iron species. *Nature* **1999**, *400* (6747), 858–861.
- Hernlem, B.; Vane, L.; Sayles, G. Stability constants for complexes of the siderophore desferrioxamine B with selected heavy metal cations. *Inorg. Chim. Acta* **1996**, *244* (2), 179–184.
- Albrecht-Gary, A. M.; Crumbliss, A. L. Coordination chemistry of siderophores: Thermodynamics and kinetics of iron chelation and release. In *Metal Ions in Biological Systems*; Sigel, A.; Sigel, H., Eds.; CRC Press: Boca Raton, FL, 1998; pp 239–316.
- Fantle, M. S.; DePaolo, D. J. Iron isotopic fractionation during continental weathering. *Earth Planet Sci. Lett.* **2004**, *228* (3–4), 547–562.
- Bergquist, B. A.; Boyle, E. A. Iron isotopes in the Amazon River system: Weathering and transport signatures. *Earth Planet Sci. Lett.* **2006**, *248* (1–2), 54–68.
- Domagal-Goldman, S. D.; Kubicki, J. D. Density functional theory predictions of equilibrium isotope fractionation of iron due to redox changes and organic complexation. *Geochim. Cosmochim. Acta* **2008**, *72* (21), 5201–5216.
- Domagal-Goldman, S. D.; Paul, K. W.; Sparks, D. L.; Kubicki, J. D. Quantum chemical study of the Fe(III)-desferrioxamine B siderophore complex—Electronic structure, vibrational frequencies, and equilibrium Fe-isotope fractionation. *Geochim. Cosmochim. Acta* **2009**, *73* (1), 1–12.
- Wiederhold, J.; Kraemer, S. M.; Teutsch, N.; Borer, P.; Halliday, A.; Kretzschmar, R. Iron isotope fractionation during proton-promoted, ligand-controlled, and reductive dissolution of goethite. *Environ. Sci. Technol.* **2006**, *40* (12), 3787–3793.
- Dideriksen, K.; Baker, J. A.; Stipp, S. L. S. Equilibrium Fe isotope fractionation between inorganic aqueous Fe(III) and the siderophore complex, Fe(III)-desferrioxamine B. *Earth Planet. Sci. Lett.* **2008**, *269* (3–4), 280–290.
- Ottoneo, G.; Zuccolini, M. V. The iron-isotope fractionation dictated by the carboxylic functional: An ab-initio investigation. *Geochim. Cosmochim. Acta* **2008**, *72*, 5920–5934.
- Jouvin, D.; Louvat, P.; Juillot, F.; Marechal, C. N.; Benedetti, M. F. Zinc isotopic fractionation: Why organic matters. *Environ. Sci. Technol.* **2009**, *43* (15), 5747–5754.
- Chen, J.; Zhang, H.; Tomuv, I.; Ding, X.; Rentzepis, P. M. Electron transfer and dissociation mechanism of ferrioxalate: A time resolved optical and EXAFS study. *Chem. Phys. Lett.* **2007**, *437*, 50–55.
- Stokey, L. Ferrozine—a new spectrophotometric reagent for iron. *Anal. Chem.* **1970**, *42* (7), 779–781.
- Arnold, G.; Weyer, S.; Anbar, A. D. Fe isotope variations in natural materials measured using high mass resolution multiple collector ICPMS. *Anal. Chem.* **2004**, *6* (2), 322–327.
- Weyer, S.; Schwieters, J. High precision Fe isotope measurements with high mass resolution MC-ICPMS. *Int. J. Mass Spectrom.* **2003**, *226* (3), 355–368.
- Roe, J. E.; Anbar, A. D.; Barling, J. Nonbiological fractionation of Fe isotopes: Evidence of an equilibrium isotope effect. *Chem. Geol.* **2003**, *195* (1–4), 69–85.

- (30) Martell, A.; Smith, R., *Critical Stability Constants*; Plenum: New York, 1989; Vol. 1, p 6.
- (31) Bigeleisen, J.; Mayer, M. G. Calculation of equilibrium constants for isotopic exchange reactions. *J. Chem. Phys.* **1947**, *15* (5), 261–267.
- (32) Urey, H. C. The thermodynamic properties of isotopic substances. *J. Chem. Soc.* **1947**, (May), 562–581.
- (33) Welch, S. A.; Beard, B. L.; Johnson, C. M.; Braterman, P. S. Kinetic and equilibrium Fe isotope fractionation between aqueous Fe(II) and Fe(III). *Geochim. Cosmochim. Acta* **2003**, *67* (22), 4231–4250.
- (34) Bullen, T. D.; White, A. F.; Childs, C. W.; Vivit, D. V.; Schulz, M. S. Demonstration of significant abiotic iron isotope fractionation in nature. *Geology* **2001**, *29* (8), 899–702.
- (35) Ludwig, K. R. *Isoplot 3.6, 3.6*; Berkeley Geochronology Center Spec. Pub: Berkeley, CA, 2008.

ES100906Z